



MINISTRY OF AVIATION

AERONAUTICAL RESEARCH COUNCIL
REPORTS AND MEMORANDA

Some Exact Calculations of the Lift and Drag
Produced by a Wedge in Supersonic Flow,
Either Directly or by Interference

By P. L. ROE

RETAIL AIRCRAFT RESEARCH
1967

LONDON: HER MAJESTY'S STATIONERY OFFICE

1967

PRICE EIGHT SHILLINGS NET

Some Exact Calculations of the Lift and Drag Produced by a Wedge in Supersonic Flow, Either Directly or by Interference

By P. L. ROE

*Reports and Memoranda No. 3478**
August, 1964

Summary.

Exact inviscid theory is applied to a simple lifting configuration consisting of a wedge beneath a plane wing, both the wedge and the wing being terminated by a trailing edge which lies along a Mach cone. The efficiency of such an arrangement is compared with the efficiency of a wedge producing lift directly through incidence, as in the Nonweiler wing. The comparison is favourable to the interference arrangement provided the parameter $M_\infty^4 C_L / \beta_\infty^2$ is less than 0.65.

In an Appendix it is shown that optimising the shape of the trailing edge makes the indirectly lifting wedge superior to the directly lifting wedge for values of $M_\infty^4 C_L / \beta_\infty^2$ between zero and unity.

LIST OF CONTENTS

1. Introduction
2. Derivation of Results for Wedge-Interference Wing
3. Analysis for Low C_L
4. An Interference Similarity Parameter
5. A Note on the 'Momentum Principle'
6. Conclusions

List of Symbols

References

Appendix

Illustrations—Figs. 1 to 10

Detachable Abstract Cards

* Replaces R.A.E. Technical Note, No. 2981—A.R.C. 26437.

Aero

LIST OF ILLUSTRATIONS

Figure

1. The wedge interference wing
 2. Configuration considered in Section 2
 3. Notation for wedge flow
 4. Derivation of equation (10)
 5. Comparison of single-shock Nonweiler and wedge-interference wings
 6. Ratios of base areas for single-shock Nonweiler and wedge-interference wings
 7. Comparison of single-shock Nonweiler and wedge-interference wings (collapsed plot)
 8. Regions of superiority of wedge-interference and Nonweiler wings
 9. Optimum wedge-interference wing
 10. Comparison of single-shock Nonweiler and optimum wedge-interference wings
-

1. Introduction

One of the simplest examples of favourable aerodynamic interference at supersonic speeds is a vertical wedge set beneath a wing (Fig. 1). The wing catches all or part of the positive pressure field generated by the wedge, and thus sustains an additional lift force. This configuration has been studied by many authors using approximate theories, for example Ferri, Clarke, and Cassaccio¹ using linear theory, and Grodzovskii² using hypersonic small perturbation theory. However, the extreme simplicity of the problem makes it easy to solve by exact inviscid theory, and the results so obtained have some interesting features.

For example, the efficiency of the interference lift produced in this way may be compared with the lift produced directly by setting a wedge at incidence. It transpires that the comparison is favourable to the interference configuration at low lift coefficients and low Mach numbers, whereas the directly lifting wedge is superior at high lift coefficients and high Mach numbers. The two effects may be combined into a single similarity parameter $M_\infty^4 C_L / \beta_\infty^2$.

It should perhaps be emphasized that there is no intention to treat this interference configuration as though it were a possible realistic aircraft shape. The aim is rather to present a family of shapes whose exact behaviour can be appreciated with the minimum of mathematics, thereby drawing attention to some features of interference effects which are not revealed by linear theory.

2. Derivation of Results for Wedge-interference Wing

The problem of a wing at zero incidence deriving lift from interference with a wedge centrebody may be treated as follows. Consider, as in Fig. 2, a tetrahedron $O A E E'$ mounted on the infinite plane xy , and symmetrically disposed with respect to a uniform free stream flowing parallel to that plane. $O A$ is perpendicular to the xy plane, in the direction of the z -axis, and has unit length. The angle EOE' is 2δ , and the angle OEA is chosen to be $\cot^{-1} \beta$, that is, the Mach angle corresponding to flow over the surface of a wedge of half-angle δ , starting from a free stream Mach number M_∞ .

An initially plane shock will spring from $O A$; let the angle which this makes with the surface $O A E$ be $\cot^{-1} B$.

From each point on the line AE will stem a Mach cone of semi-angle $\cot^{-1} \beta$. The region of flow between the shock and the envelope of these cones will be two-dimensional and hence calculable.

Now consider the point on AE whose co-ordinates are $(x_o, 0, 1 - x_o/\beta)$.

The equation of the Mach cone from this point is:

$$y^2 + (z - 1 + x_o/\beta)^2 = (x - x_o)^2/\beta^2. \quad (1)$$

It is easily shown that where these cones intersect the plane $z = 0$, the cone from A lies ahead of all the other cones, except at the point E , where they all meet. Thus the rearward boundary of two dimensional flow on the plane is obtained by setting $x_o = 0, z = 0$, in equation (1),

i.e.

$$\beta^2(y^2 + 1) = x^2 \quad (2)$$

which is a hyperbola.

Let this hyperbola cut OS in T , and choose $OEHT$ to be the 'wing' surface. If suffix(_s) refers to the shock, suffix(_c) to the trace EHT of the Mach conoid, and if the co-ordinates of T are $x = x_T = By_T$, $y = y_T$, then the area of this single wing panel is S , where

$$S = \int_0^{y_T} (x_c - x_s) dy \quad (3)$$

$$= \beta \int_0^{y_T} (1 + y^2)^{\frac{1}{2}} dy - \int_0^{y_T} By dy$$

$$= \beta \left[\frac{y}{2} (1 + y^2)^{\frac{1}{2}} + \frac{1}{2} \ln \{ y + (1 + y^2)^{\frac{1}{2}} \} \right]_0^{y_T} - \frac{By_T^2}{2}$$

$$= \frac{x_T y_T}{2} + \frac{\beta}{2} \ln \left(y_T + \frac{x_T}{\beta} \right) - \frac{By_T^2}{2}$$

$$= \frac{\beta}{2} \ln \left(y_T + \frac{x_T}{\beta} \right)$$

$$= \frac{\beta}{2} \ln \left[\frac{y_T(\beta + B)}{\beta} \right]. \quad (4)$$

Substituting $x = By$ in equation (2) yields

$$y_T^2 = \frac{\beta^2}{B^2 - \beta^2}$$

and putting this into (4) gives

$$S = \frac{\beta}{4} \ln \left[\frac{y_T^2(\beta + B)^2}{\beta^2} \right] = \frac{\beta}{4} \ln \left[\frac{\beta + B}{B - \beta} \right] \quad (5)$$

If we choose a free stream Mach number and a wedge angle, both B and β may be obtained from the standard charts of flow over wedges. Since we also know the planform area of the body $OEE' = \beta^2 \sin \delta \cos \delta$, and the base area (which is the forward projection of AEE') $= \beta \sin \delta$, we can exactly evaluate the performance of the configuration in inviscid flow. The results of such analysis are shown in Figs. 5a, b and c, for free-stream Mach numbers of 2.0, 4.0 and 8.0.

Also shown on these graphs are the performances of Nonweiler wings⁴, which are equivalent to those of plane wedges; it will be noted that these are superior to the interference arrangement at high values of M_∞ or C_L , and inferior at low values.

In both cases the coefficients are based on total projected planform area, and pressures on the base and on the upper surface have been taken equal to free stream.

It may be noted here that, for given M_∞ and C_L , the ratio of wetted area to planform area is fixed for the particular interference configuration studied here. For the Nonweiler wing this ratio may take on any value between unity and infinity, depending on the anhedral angle, but for 'realistic' Nonweiler shapes it normally has a value which is slightly less than that for the interference wing. Hence the skin friction-drag will tend to be slightly larger on the interference wing.

The ratio of base area to planform area is shown in Fig. 6 for both types of wing.

3. Analysis for Low Lift Coefficients.

The parameter C_L^2/C_D is always finite for a Nonweiler wing, but for the interference wing it has a logarithmic singularity at $C_L = 0$. The purpose of the present section is to determine the asymptotic form of the curve near this singularity, which will be made the basis of a similarity rule.

If δ is small, both B and β will be close to β_∞ , so that we may approximate to equation (5) by

$$S = \frac{\beta_\infty}{4} \ln \left[\frac{2\beta_\infty}{B-\beta} \right]. \quad (6)$$

Now

$$B-\beta \equiv (B-\beta_\infty) - (\beta-\beta_\infty) = (B-\beta_\infty) - d\beta.$$

Since

$$M_\infty dM = \beta_\infty d\beta$$

and since for small δ we can use the isentropic relationship

$$dM = -\frac{M_\infty}{\beta_\infty} \left(1 + \frac{\gamma-1}{2} M_\infty^2 \right) \delta \quad (8)$$

we have

$$d\beta = -\frac{M_\infty^2}{\beta_\infty^2} \left(1 + \frac{\gamma-1}{2} M_\infty^2 \right) \delta \quad (9)$$

From Fig. 3 we have

$$B = \cot(\mu_\infty - \delta + \epsilon).$$

Therefore (see Fig. 4)

$$B - \beta_\infty = (\varepsilon - \delta) \left(\frac{d(\cot\theta)}{d\theta} \right)_{\theta=\mu} = (\delta - \varepsilon) M_\infty^2. \quad (10)$$

But from Ref. 3, p. 93, for small δ

$$\varepsilon = \frac{\gamma+1}{4} \frac{M_\infty^2}{\beta_\infty^2} \cdot \delta. \quad (11)$$

Combining (10) and (11)

$$B - \beta_\infty = \left[1 - \frac{\gamma+1}{4} \frac{M_\infty^2}{\beta_\infty^2} \right] M_\infty^2 \delta. \quad (12)$$

Combining (7), (9) and (12)

$$B - \beta = \frac{M_\infty^4}{\beta_\infty^2} \frac{\gamma+1}{4} \cdot \delta. \quad (13)$$

Substituting this into (6), the area of one wing panel influenced by a narrow wedge is

$$S = \frac{\beta}{4} \ln \left[\frac{8\beta_\infty^3}{M_\infty^4 (\gamma+1) \delta} \right]. \quad (14)$$

Now for sufficiently small δ we may neglect the body planform area with respect to the wing area, and take $C_L = C_p = 2\delta/\beta_\infty$. In this way we obtain

$$\frac{C_L^2}{C_D} = \frac{1}{\beta_\infty} \cdot \ln \left[\frac{16\beta_\infty^2}{(\gamma+1) M_\infty^4 C_L} \right]. \quad (15)$$

This, then, is the asymptotic form of the curves of Fig. 5 near $C_L = 0$. Due to a fortunate cancelling of errors it is found that equation (15) represents the exact curve over quite a large range of C_L (see Figs. 5a and b especially).

For Nonweiler wings, linear theory predicts simply

$$\frac{C_L^2}{C_D} = \cot \delta C_L = \frac{2}{\beta_\infty}.$$

The non-linear effects can be represented to first order by the following expression, which is obtained from the oblique-shock relationships by suitable simplification

$$\frac{C_L^2}{C_D} = \frac{2}{\beta_\infty} \left[1 + \frac{(\gamma+1)}{8} M_\infty^2 C_L \right]. \quad (16)$$

4. An Interference Similarity Parameter

In Ref. 2 Grodzovskii quotes results which, when put into the notation of this report, give M_∞ large and δ small,

$$B = \frac{2}{(\gamma-1)\delta}$$

$$\beta = \frac{1}{\delta} \left(\frac{2}{\gamma(\gamma-1)} \right)^{\frac{1}{2}}$$

$$C_p = (\gamma+1)\delta^2.$$

Using these it is easily shown that, with $\gamma = 7/5$

$$\frac{C_L^2}{C_D} = 0.258 C_L^{\frac{1}{2}}.$$

Multiplying the left-hand side by β_∞ , and the right-hand side by M_∞^2/β_∞ , for when M_∞ is large these will be nearly equal, and rearranging

$$\beta_\infty \frac{C_L^2}{C_D} = 0.258 \left(\frac{M_\infty^4 C_L}{\beta_\infty^2} \right)^{\frac{1}{2}}. \quad (18)$$

Comparing this with equation (15), we see that within the range of applicability of either equation, $\beta_\infty C_L^2/C_D$ is a function only of the combined variable $M_\infty^4 C_L/\beta_\infty^2$. This leads us to expect that the exact results of Figs. 5a, b and c may collapse onto a single curve if plotted in this form, and this is seen to be the case in Fig. 7.

Moreover, we may rewrite equation (16), which gives the performance of Nonweiler wings at small C_L , in the form

$$\beta_\infty \frac{C_L^2}{C_D} = 2 \left[1 + \frac{(\gamma+1)}{2} \left(\frac{\beta_\infty^2}{M_\infty^2} \right) \frac{M_\infty^4 C_L}{\beta_\infty^2} \right] \quad (19)$$

Thus, if we plot Nonweiler wings in the same way, we shall obtain a family of lines which intersect the vertical axis in the same point, but depart from it with slopes which are all small, and differ only in the factor $\beta_\infty^2/M_\infty^2$. This is also done in Fig. 7.

Fig. 7 now shows that the relative merits of directly and indirectly lifting wedges depend only on the parameter $M_\infty^4 C_L/\beta_\infty^2$. The interference arrangement is superior if this is less than about 0.65, and *vice versa*.

Fig. 8 shows how, using this result, the M_∞, C_L plane may be divided into two regions by the line $C_L = 0.65 \beta_\infty^2/M_\infty^4$. Above this line the Nonweiler wing is the better of the two. The greatest range of lift coefficients over which the wedge-interference wing is better occurs at $M_\infty = \sqrt{2}$. This is also the Mach number at which, for given C_L , the ratio $(L/D)_{W.I.W.}/(L/D)_{N.W.}$ is maximum. Physically this corresponds to the fact that, for given wedge angle, this is the Mach number for which the characteristics behind the shock are most nearly parallel to the shock wave itself, so that the maximum area is available for the interference lift to act on. This result may be proved by differentiating equation (13).

5. *A Note on the 'Momentum Principle'*⁵

It is interesting to consider the changes of momentum produced by the two types of wing. Nonweiler wings produce locally only downward momentum and the wedge-interference wing only sideways momentum. (This must, of course, be converted to downward momentum in the wake.) At first sight it would seem that the Nonweiler wing operates in the more efficient manner. It has just been shown, however, that under certain circumstances the interference arrangement is the more efficient lifting device. This example serves to show that the attempt to derive efficient lifting shapes by simple arguments based on 'near field' momentum considerations, as was done for example by Eggers and Syvertson in Ref. 5, can be misleading.

6. *Conclusions*

It would, of course, be quite unsound to draw firm general conclusions from a limited analysis of two rather artificial configurations, but it is both tempting and plausible to regard these two designs as typical of two extreme classes of lifting shapes. In the Nonweiler wing, every element of the surface develops the same lift and drag as would a simple wedge having the same inclination to the free stream. In the wedge-interference wing, by contrast, neither component in isolation would develop any lift at all. Thus the two designs may be regarded as typical of lifting surfaces which derive either very little or most of their lift from the interference between different parts. The function $M_\infty^4 C_L / \beta_\infty^2$ then may be regarded as a similarity parameter related to the extent to which interference may be incorporated as a useful feature of a design.

LIST OF SYMBOLS

x, y, z	Cartesian coordinates defined in Fig. 4
B	Cotangent of angle between wedge and shock
C_L, C_D	Coefficients of lift and drag based on total projected planform area
M	Mach number
S	Area of wing panel
β	$(M^2 - 1)^{\frac{1}{2}}$
γ	Ratio of specific heats
δ	Wedge semi-angle
ε	Angle between shock and free-stream Mach direction
μ	$\sin^{-1} 1/M$
<i>Subscripts</i>	
(∞)	Denotes free-stream conditions
(c)	Conditions on Mach conoid <i>EHT</i> of Fig. 2
(s)	Conditions on shock wave
(T)	co-ordinates of wing tip

REFERENCES

- | <i>No.</i> | <i>Author(s)</i> | <i>Title, etc.</i> |
|------------|---|--|
| 1 | A. Ferri, J. H. Clarke,
A. Cassaccio | .. Drag reduction in lifting systems by advantageous use of interference.

PIBAL Rept. No. 272, May, 1955. |
| 2 | G. L. Grodzovskii | Useful interference of a wing fuselage at hypersonic speeds.
<i>Izv. Akad. Nauk. SSSR. Otd. Tekhn. N. Mekh. i Mash.</i> No. 1, pp. 170-173, 1959. |
| 3 | H. W. Liepmann, A. Roshko | <i>Elements of gasdynamics.</i>
John Wiley & Sons, 1957. |
| 4 | T. R. F. Nonweiler | Delta wings of shapes amenable to exact shock wave theory.
<i>J.R. Ae.S.</i> 67 (625), January, 1963. |
| 5 | A. J. Eggers, C. R. Syvertson | Aircraft configurations developing high lift-drag ratios at high supersonic speeds.
NACA RM A55 LO5, 1956. |
| 6 | J. Pike | The analytical performance of lifting surfaces supporting plane shock waves.
A.R.C. 28452. |

APPENDIX

The Optimum Wedge-Interference Wing

In the main body of this report the trailing edge of the wedge-interference wing is taken to be simply the trace of a Mach cone. However, by suitably modifying the trailing edge it is possible to improve the performance.

In this Appendix the results of optimizing the trailing edge are briefly described.

Since all the lift is produced by a constant pressure acting on the wing, and all the drag by the same constant pressure acting on the body, best performance for given wedge angle is achieved by maximizing the ratio (wing area):(body area). The restriction must be observed, however, that uniform flow is possible over the whole of the chosen areas. This may be interpreted geometrically as follows:

Lemma 1

It must not be possible to find any two points on the trailing edge such that the straight line joining them in space makes an angle less than $\cot^{-1}\beta$ with the direction of the flow behind the shock. This is a necessary and sufficient condition.

Lemma 2

Any line drawn in a plane which is tangent to a Mach cone makes an angle with the flow direction which is greater than or equal to $\cot^{-1}\beta$

Refer now to Fig. 9a. This shows the original wing shape $AEHTOA$. We wish to modify the trailing edge $AEHT$ so as to increase the ratio of wing area to body area. Let the new trailing edge be $ABNWM$. Consider the projection of Fig. 9a onto a plane normal to the Mach line AT . (Fig. 9b. In this projection MWN must lie entirely on the same side of ABN as does the point O , since otherwise *Lemma 1* is not satisfied. Therefore we have the inequality,

$$\frac{\text{area } MNO}{\text{area } ANO} \leq \frac{\sin \gamma_1}{\sin \gamma_2}$$

where γ_1, γ_2 , are the angles made by AT with the planes ANO and MNO respectively.

Now consider the plane which is tangent along AT to the Mach cone from A . This appears as the line AP in Fig. 9b. Choose the intersections AP, PT of this plane with the body and wing surfaces to be the trailing edge as in Fig. 9c. *Lemma 2* shows that such a trailing edge meets the requirements of *Lemma 1*. Since Fig. 9b shows

$$\frac{\text{area } TPO}{\text{area } APO} = \frac{\sin \gamma_1}{\sin \gamma_2} \tag{A.1}$$

it follows that $APTOA$ is an optimum wing. It may also be shown without difficulty that it is a unique optimum.

Its performance can be found in an exactly similar manner to that used for the non-optimum wing in Sections 2 to 4. Here we shall quote results without proof.

$$\left(\frac{L}{D}\right)_{\text{opt}} = \frac{\beta \operatorname{cosec} \delta}{(B^2 - \beta^2)^{\frac{1}{2}}} \text{ exactly} \tag{A.2}$$

For small wedge angles and moderate Mach numbers, we have, analogously to equation (15),

$$\left(\frac{C_L^2}{C_D}\right)_{\text{opt}} = \frac{1}{\beta_\infty} \left(\frac{-16\beta_\infty^2}{(\gamma+1)M_\infty^4 C_L} \right)^{\frac{1}{2}} \tag{A.3}$$

For small wedge angles and hypersonic Mach numbers

$$\begin{aligned} \left(\frac{C_L^2}{C_D}\right)_{\text{opt}} &= \left[\frac{\gamma(\gamma-1)^2}{\gamma^2+1}\right] C_L^{\frac{1}{2}} \\ &= 0.275 C_L^{\frac{1}{2}} \text{ if } \gamma = 7/5. \end{aligned} \tag{A.4}$$

From equations (A.3) and (A.4) we deduce that the same similarity parameters ($\beta_\infty C_L^2/C_D$) and ($M_\infty^4 C_L/\beta_\infty^2$) will serve to unify the results for optimum wings, which are plotted in Fig. 10. The improvement is seen to be quite substantial, and the criterion which determines whether the directly or indirectly lifting wedge is superior is now whether ($M_\infty^4 C_L/\beta_\infty^2$) is greater or less than unity.

Wedge-interference wings and single-shock Nonweiler wings are both special cases of wings supporting plane shock waves. A full theoretical study of the general case has been provided by Pike⁶, who studies, amongst other things, the optimum orientation of the shock waves in space. The similarity parameter $M_\infty^4 C_L/\beta_\infty^2$ is also found to be of significance in the optimization of these more general shapes.

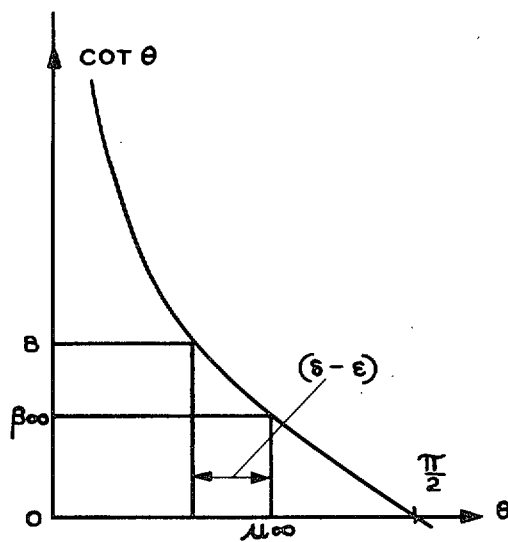


FIG. 4. Derivation of equation (10).

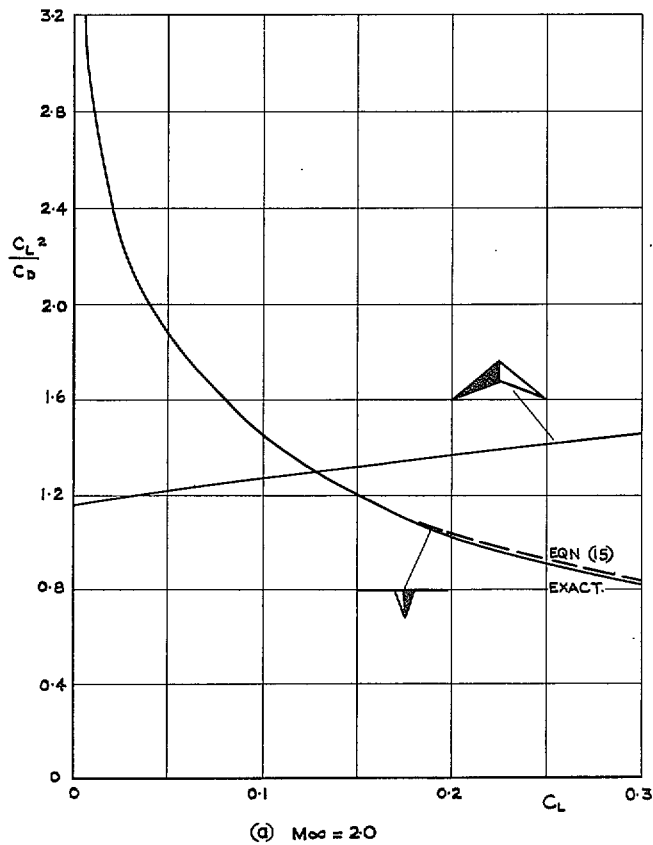


FIG. 5. Comparison of single-shock-Nonweiler and wedge-interference wings.

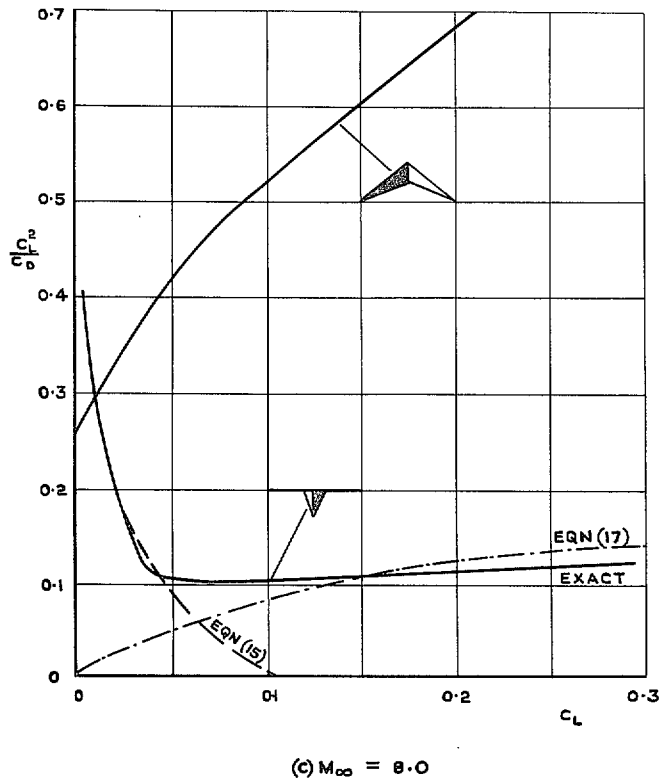
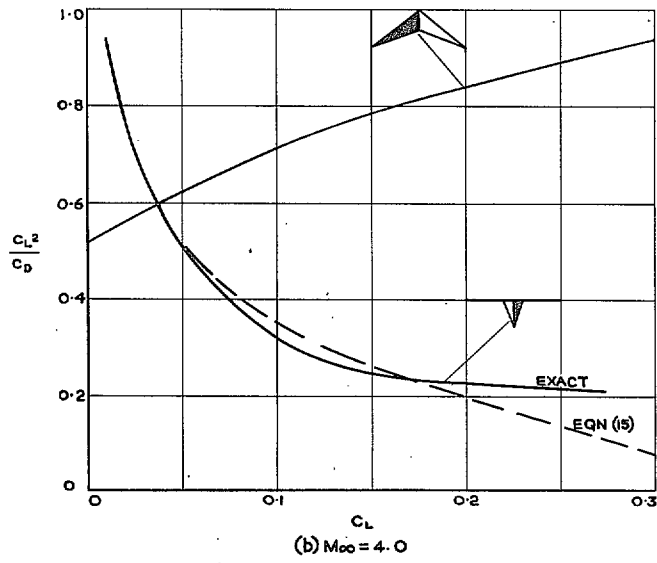


FIG. 5 (cont.). Comparison of single-shock-Nonweiler and wedge-interference wings.

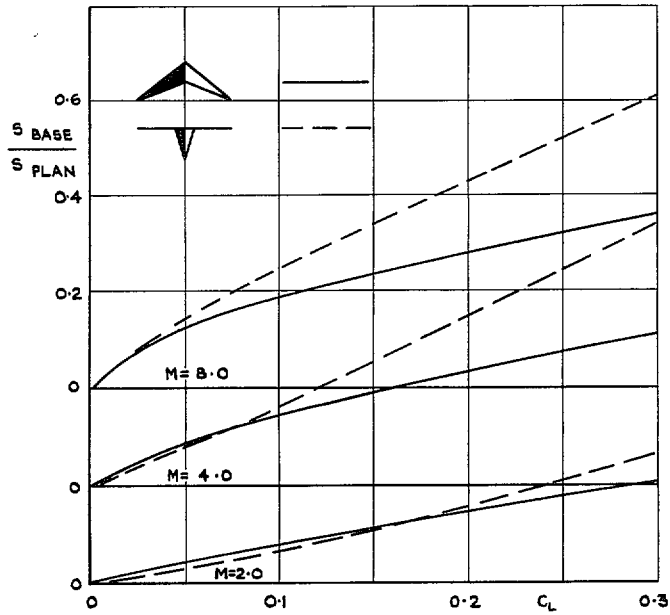


FIG. 6. Ratios of base areas for single shock Nonweiler and wedge-interference wings.

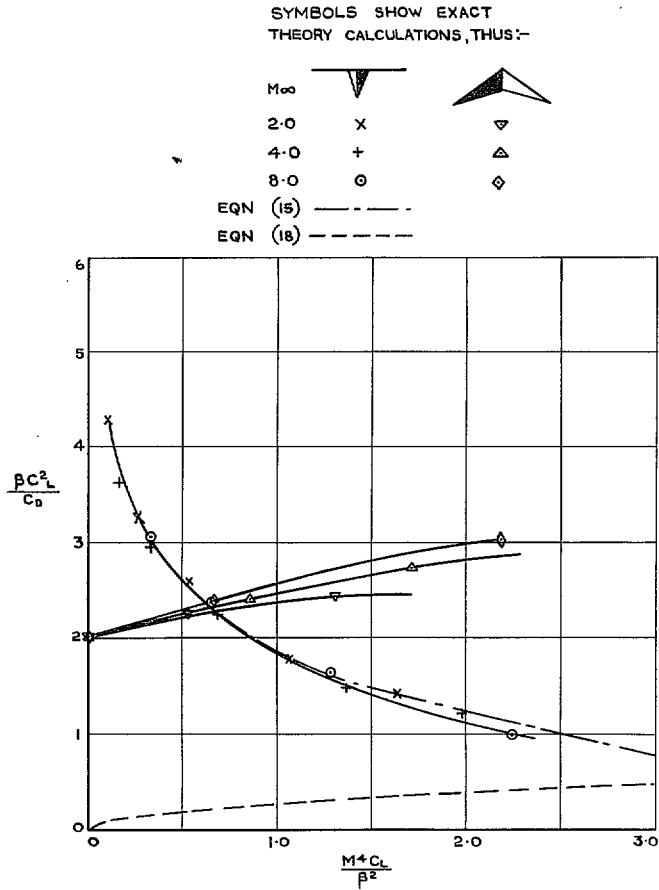


FIG. 7. Comparison of single-shock Nonweiler and wedge-interference wings (collapsed plot).

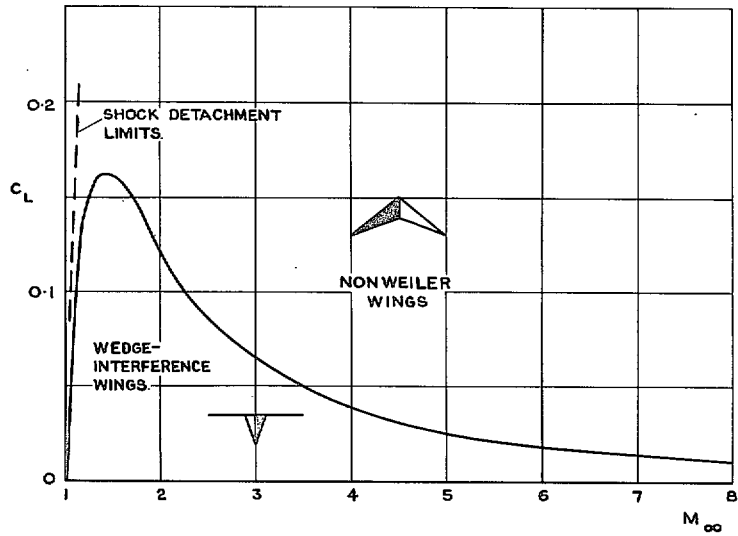


FIG. 8. Regions of superiority of wedge-interference and Nonweiler wings.

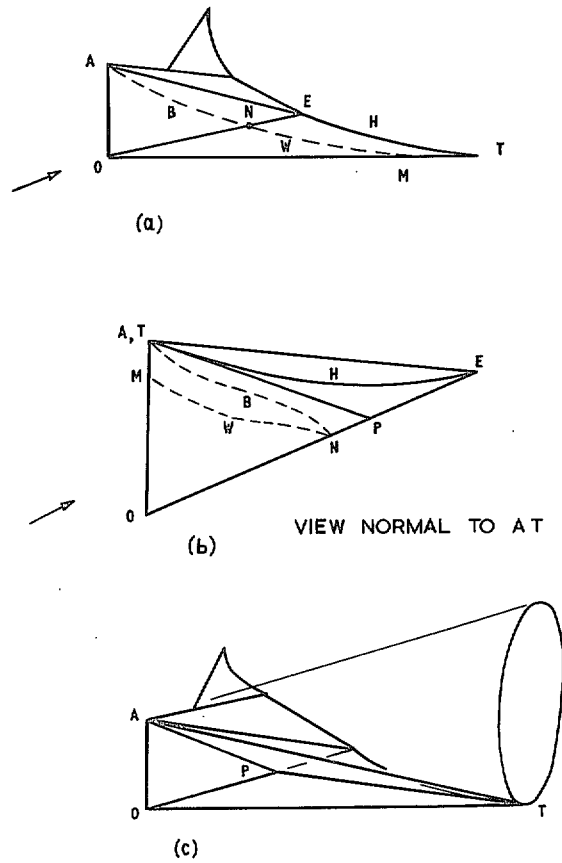




FIG. 9. Optimum Wedge-Interference Wing.

SYMBOLS SHOW EXACT THEORY CALCULATIONS THUS:-

M_{∞}		
2	X	▽
4	+	△
8	○	◇

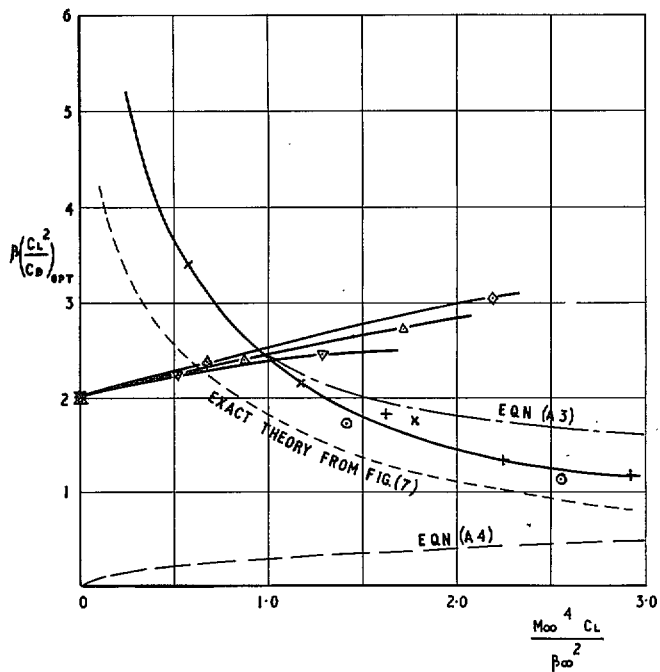


FIG. 10. Comparison of Single-Shock nonveiler and optimum Wedge-Interference Wings.

© *Crown copyright* 1967

Published by
HER MAJESTY'S STATIONERY OFFICE

To be purchased from
49 High Holborn, London w.c.1
423 Oxford Street, London w.1
13A Castle Street, Edinburgh 2
109 St. Mary Street, Cardiff
Brazennose Street, Manchester 2
50 Fairfax Street, Bristol 1
35 Smallbrook, Ringway, Birmingham 5
7-11 Linenhall Street, Belfast 2
or through any bookseller